SINGLE-RESONATOR, TIME-SWITCHED FM MEMS ACCELEROMETER WITH THEORETICAL OFFSET DRIFT COMPLETE CANCELLATION

Cristiano R. Marra[1], Filippo M. Ferrari[1], Saleh Karman[1], Alessandro Tocchio[2], Francesco Rizzini[2] and Giacomo Langfelder[1]

[1]Dipartimento di Elettronica, Informazione e Bioingegneria, Politecnico di Milano, ITALY and [2]ST Microelectronics, Cornaredo (MI), ITALY

ABSTRACT

The work presents the first frequency modulated (FM) accelerometer operating in time-switched differential mode: readout is based on a double sampling of the oscillation frequency of a single resonator, consecutively biased in two different configurations in time. This technique theoretically enables zeroing of offset drift components related to the temperature coefficient of frequency (TCf), even in presence of process nonuniformities.

Additionally, the TCf offset drift component can be tuned to compensate the thermal-stress component, delivering compact, ultra-low-drift, accelerometers. Experiments on various samples demonstrate repeatable sub-50µg/K drift without post-acquisition corrections, at a consumer-grade 100µg/√Hz noise density.

INTRODUCTION

Emerging next-generation consumer applications (as pedestrian navigation and mixed reality) are making urgent the availability of low-cost, high-accuracy MEMS inertial sensors. For what concerns MEMS accelerometers, a critical issue is represented by the ZGO (zero g offset) stability with respect to environmental changes. Offset thermal stability for 16-g-full-scale-range (FSR) capacitive MEMS accelerometers reaches values around 1 mg/K [1], out of target for innovative applications. Improved stability can be achieved only at the cost of lower FSR.

Frequency-modulated (FM) accelerometers have been studied as an alternative to capacitive solutions, mainly for their high-dynamic range and for the quasi-digital nature of their frequency output [2, 3, 4]. In recent implementations FM MEMS accelerometers demonstrated robust environmental stability [5, 6], reaching thermal offset drifts as low as 120µg/K. However, such results were shown on single samples, and without a conceptual basis that guarantees the drift value to be held regardless of process nonuniformities. Furthermore, these solutions were not conceived to be compatible with typical consumer constraints in terms of area and power dissipation.

This work presents a novel FM MEMS accelerometer that, through a newly introduced time-switched working principle, is capable to reach superior performances in terms of offset thermal drift with respect to the state of the art, though keeping area, expected power consumption and resolution fully compatible with consumer requirements.

DEVICE DESCRIPTION

Thermal drift in FM accelerometers

Resonant accelerometers are usually constituted by a pair of MEMS resonators, whose frequency varies differentially if an external acceleration a_{ext} is acting on the inertial mass. The information about the input acceleration is recovered from the resonators frequency difference:

$$f_{out} = f_2 - f_1 = f_{0,2} - f_{0,1} + 2 \cdot \Delta f(a_{ext}) \qquad (1)$$

where $2 \cdot \Delta f(a_{ext})$ is the differential output frequency variation, related to accelerations through a scale factor S, while $f_{0,1}$ and $f_{0,2}$ are the resonant frequencies at rest (i.e. for $a_{ext} = 0$) of the two MEMS resonators, at a reference temperature T_0. By definition, the ZGO of a resonant accelerometer is the difference between the two $f_{0,i}$ divided by S, and its thermal behavior depends on the thermal drift of each resonating element.

Indeed, it is well-known that a polysilicon MEMS resonator, under a temperature change, varies its resonant frequency linearly with the Young's Modulus temperature coefficient ($TCE \approx -60ppm/K$):

$$\frac{df_{0,i}}{dT} = f_{0,i} \cdot \frac{TCE_i}{2} \qquad (2)$$

Consequently, the ZGO thermal drift of a resonant accelerometer can be written as follows:

$$\frac{dZGO}{dT} = \frac{1}{S} \cdot \left(f_{0,2} \cdot \frac{TCE_2}{2} - f_{0,1} \cdot \frac{TCE_1}{2} \right) \qquad (3)$$

Thus, the offset thermal drift is determined by $f_{0,i}$ and TCE_i mismatches among the different oscillating elements. This contribution apparently benefits from a scale factor increase but, generally, high sensitivities are obtained when fabricating resonators with small critical dimensions [3], degrading their precise frequency matching in presence of process tolerances.

Consequently, even though the TCE mismatch can be minimized with the physical proximity of the resonators [5], the rest frequency mismatch remains an unavoidable contribution to the offset drift.

Description of the novel approach

This work conceptually overcomes the drift problem by using a differential readout operated *in time on a single resonator*, rather than *in space on two separate resonators*. The principle enables, even in presence of process nonidealities, to null TCf-related contributions of Eq. (3).

The proposed in-plane accelerometer is represented in Fig. 1. The suspended structure is enclosed by an external rigid frame with centered anchors to optimize rejection of process-dependent thermal stress, resulting in a total active area of $(510\mu m)^2$. The sensor is split into two symmetric halves, connected by two 4-fold tuning-fork springs. Each half features a proof rotor suspended by four 4-fold springs, two sets of combs and two sets of tuning-plate ports.

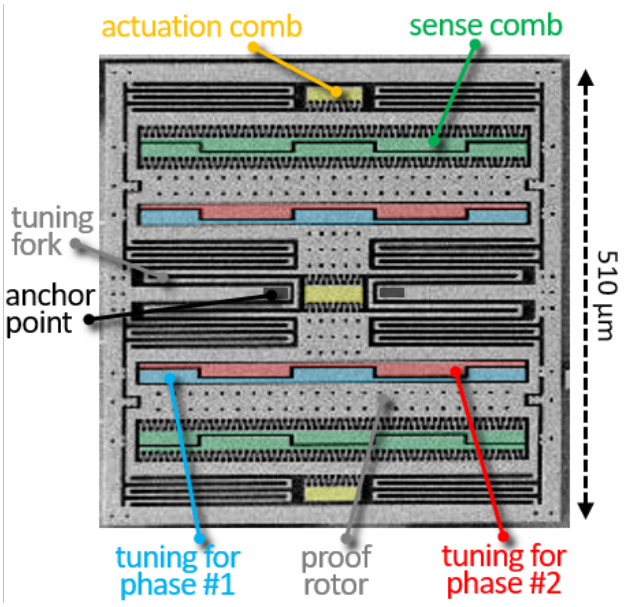

Figure 1: SEM top view, with highlighted actuation and pick off combs for anti-phase excitation, parallel-plate tuning electrodes, rotor proof frame and anchor points.

In operation, the sensor is kept in antiphase resonance oscillation at f_0 = 25 kHz (the finite element modal shape is shown in Fig. 2a) by comb-based push-pull actuation and differential pick-off. Accelerations cause instead in-phase motion (see Fig. 2b), and displace the rotor by a common-mode displacement towards either tuning port #1 or #2.

These parallel-plate ports operate in complementary mode. During a first interval ΔT_1 (named phase #1) electrode #1 is biased at a DC voltage V_{tun}, while electrode #2 is kept equipotential with the rotor: only the former gives a contribution in terms of electrostatic softening.

Supposing that the external acceleration is directed in such a way to impress an in-phase movement to the proof mass towards electrode #1, the anti-phase frequency results reduced with respect to the rest value f_0 as follows:

$$f_1 = \frac{1}{2\pi} \cdot \sqrt{\frac{k_{mec} - k_{el,0} - k_{el}(a_{ext})}{m}}, \quad t \in \Delta T_1 \qquad (4)$$

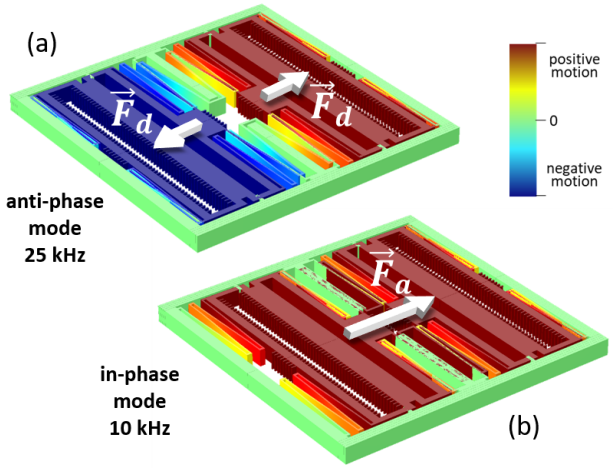

Figure 2: finite element simulation results showing the anti-phase (a) and the acceleration sensitive (b) modes.

where m is the mass associated with the anti-phase motion, k_{mech} is the mechanical contribution to the overall anti-phase stiffness, $k_{el,0}$ is the rest value of the electrostatic portion of the overall stiffness and $k_{el}(a_{ext})$ is its shift due to the external stimulus.

In the immediately following time interval ΔT_2 (named phase #2), the voltages applied on the tuning ports are switched. In this situation, supposing the external acceleration unchanged, the rotor mass moves away from the active tuning port #2, and thus the resonant frequency results increased (with respect to the rest value) and equals:

$$f_2 = \frac{1}{2\pi} \cdot \sqrt{\frac{k_{mec} - k_{el,0} + k_{el}(a_{ext})}{m}}, \quad t \in \Delta T_2 \qquad (5)$$

Subtracting the two frequency samples acquired during phase #1 and phase #2 gives rise to a differential readout.

It should be noted that, in the proposed accelerometer, the tuning phase temporization is easily managed, just by driving the tuning ports with two anti-phase square-waves. The obtained output can be thus described, using a 1st-harmonic approximation and a 1st-order linearization as:

$$f_{out} = f_0 + (f_2 - f_1) \cdot \sin(2\pi f_{sw} t) \qquad (6)$$

According to the sampling theorem, the switching frequency f_{sw} should be set at least at twice the desired signal bandwidth (e.g. f_{sw} = 100 Hz copes with a 50 Hz bandwidth). Note how this FM modulation of the output signal bypasses slow temperature drifts of the anti-phase frequency f_0.

Residual offset trimming

The proposed methodology completely erases the TCf-related offset thermal drift contribution in the ideal case of proof mass perfectly centered between the two tuning ports at rest. Indeed, in this case the term $k_{el,0}$ in Eq. (4-5) yields the same value. In a more realistic situation, due to process residual stresses and fabrication tolerances, the rotor has an initial in-phase displacement even in absence of external accelerations, resulting in a non-null ZGO. In this situation, being the rotor gap from the two tuning ports different, also $k_{el0,i}$ in Eq. (4-5) results different.

Since the temperature coefficient of a resonator is by definition $TCf = (df_0/dT)/f_0$, one can derive its expression for each of the tuning phases:

$$TCf_i = \frac{TCE}{2} \cdot \frac{1}{1 - \frac{k_{el,0i}}{k_{mec}}} \qquad (7)$$

Consequently, the TCf-related thermal drift presents a residual contribution equal to:

$$\frac{dZGO}{dT} = \frac{1}{S} \cdot \frac{TCE}{2} \left(f_{0,2} \frac{1}{1 - \frac{k_{el,02}}{k_{mec}}} - f_{0,1} \frac{1}{1 - \frac{k_{el,01}}{k_{mec}}} \right) \qquad (8)$$

This residual ZGO drift can be finely zeroed slightly

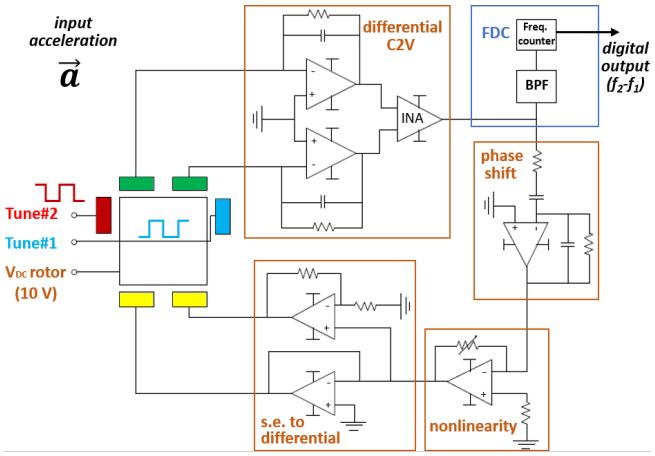

Figure 3: system view including the sensor with switched tuning signals, the sustaining oscillator and the off-the shelf frequency to digital converter.

unbalancing the tuning waves, resulting in a re-centering of the proof mass. Furthermore, it is interesting to note (i) that this contribution can be amplified on purpose, with a selectable sign, so to counterbalance thermal drifts related to other sources (e.g. process-related thermal stresses in suspensions); and (ii), that the contribution related to TCE_i mismatches in FM accelerometers relying on differential resonators (Eq. (3)) is intrinsically eliminated.

EXPERIMENTAL RESULTS

System overview

The anti-phase mode is kept in oscillation by a discrete-component electronic board, as schematized in Fig. 3. The motional current generated by the proof mass oscillation is converted into a voltage output by a differential charge amplifier stage, and then to a single ended signal by an instrumentation amplifier (INA). The Barkhausen criterion on loop phase is satisfied sending the INA output to an analog 90° shifter, while a high-gain stage ensures a fast start-up and provides the nonlinearity once the regime conditions is reached. Finally, a push-pull driving is achieved through a pair of inverting/non-inverting buffers.

Frequency readout is carried out sending the INA output to an off-the shelf Keysight frequency meter, previously band-passed in order to cut-off wide-band noise at the instrument input, thus avoiding noise folding issues related to this specific measurement methodology.

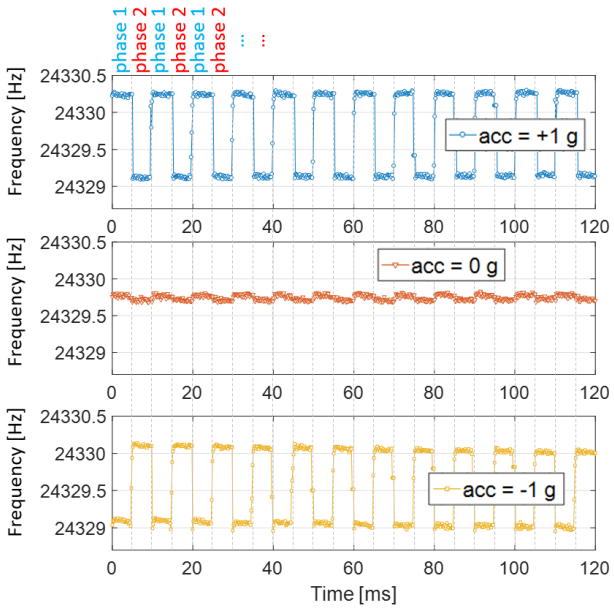

Figure 4: time traces of the measured frequency output under [-1, 0, 1] g constant accelerations.

Device characterization

A first validation of the device working principle is provided by tilting the board in order to invert the sign of gravity acceleration applied to the accelerometer. Figure 4 reports the time traces of measured frequencies under constant accelerations of [+1, 0, -1] g, for 24 consecutives, 5-ms-switching phases (f_{sw} = 100 Hz). It can be observed that, for the same input acceleration, the frequency shift with respect to the rest value is opposite in sign in the two temporal phases: the difference between the two shifts is proportional to acceleration. A residual offset of about 50 mg is visible under no accelerations.

Larger excitations were applied by mounting the electronic board on a rate table, with the MEMS sensor displaced from the rotation center, in order to exploit centrifugal accelerations. In this condition, the proof mass was subject to accelerations ramping from *0 g* to *8 g*. Figure 5 reports the obtained scale factor of *1.02 Hz/g*, at the same

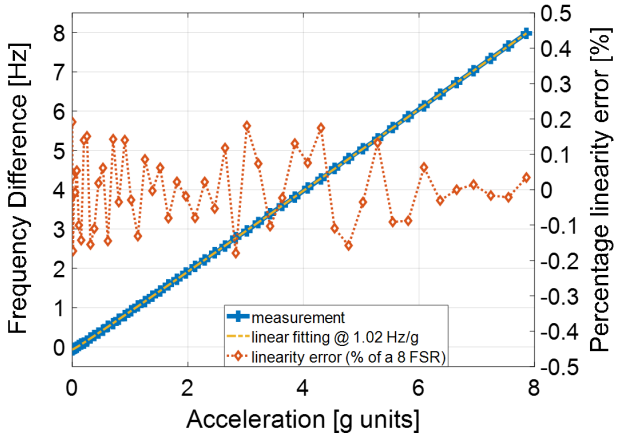

Figure 5: response to acceleration up to 8 g, showing obtained scale factor and negligible linearity error.

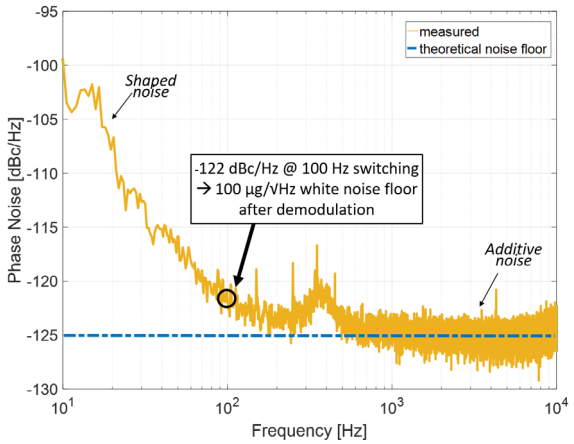

Figure 6: measured output phase noise, corresponding to 100 µg/√Hz, close to the expected noise floor.

time demonstrating sub-*0.2%* linearity errors. Finally, phase noise characterization (Fig. 6) of the electronic oscillator shows a phase noise level of *-122 dBc/Hz* for *100-Hz* switching tuning waves, corresponding to an equivalent input acceleration noise density of 100 µg/√Hz, compatible with consumer application specifications.

ZGO thermal drift

Offset thermal drift measurements are carried out mounting the electronic board coupled with the device orthogonal to the gravity direction, inside a climatic chamber. The chamber is pre-heated at 95° and turned off to avoid measuring vibrations of the instrument. The cooling down is monitored through a temperature sensor positioned close to the MEMS. Zero-g offset values are captured for each degree Celsius change.

As the MEMS device was directly wire-bonded on the PCB board to minimize parasitics, in order to check the repeatability of thermal stability performances, three different sensors on three different boards were assembled and tested with the described procedure.

Figure 7 reports measured offset drifts for these three systems, and shows how all samples reach sub-50 µg/K thermal coefficient, without any post-process compensation after direct data (frequency) acquisition.

CONCLUSIONS

The work presented the first single-resonator, time-switched, ultra-low-drift FM MEMS accelerometer. The sensor is conceived to cope with consumer constraint in terms of area and noise density. For what concerns the expected power consumption, it can be noted that the output frequency modulation of Eq. (6) is conceptually identical to the one achieved in a Lissajous FM gyroscope [7, 8]. Thus, the sensor can be coupled with low-power, low-phase noise electronic oscillators [9] and frequency to digital converters [10] already conceived for this kind of sensor, with an interesting perspective of an all-FM-sensor 6-DOF MEMS inertial measurement unit.

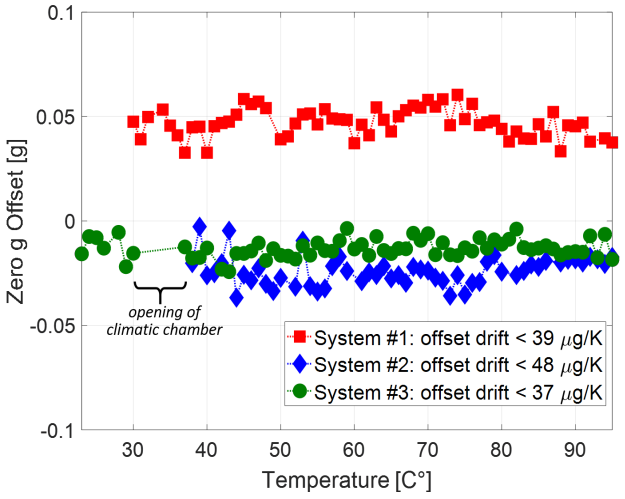

Figure 7: drift on three sensors measured from 95°C down to room temperature. Fitting coefficients are <50µg/K (the actual, likely lower value is masked by added noise associated to the complicated setup mounted inside the climatic chamber).

Furthermore, through the achievement of a differential readout on a single resonator, thanks to the time-switched operation, the TCf-related offset drift can be erased or finely tuned to counterbalance other thermal drift sources. In this way, the sensor achieves repeatable sub-50 µg/K ZGO drift, a big step towards the realization of navigation-grade consumer MEMS accelerometers.

REFERENCES

[1] Invensense, ICM-20600 High Performance 6-Axis MEMS Motion Tracking Device, www.invensense.com, Oct 2016.

[2] T.A. Roessig, R.T. Howe, A.P. Pisano, and J. H. Smith, "Surface-micromachined resonant accelerometer". in *Digest Tech. Papers IEEE Transducers-1997,* Chicago, June 1997, vol. 2, pp. 859-862.

[3] X. Zou and A. A. Seshia "A high-resolution resonant MEMS accelerometer." in *Digest Tech. Papers IEEE Transducers-2015,* Anchorage, June 21-25, 2015, pp. 1247-1250.

[4] C. Comi, A. Corigliano, G. Langfelder, A. Longoni, A. Tocchio and B. Simoni "A resonant microaccelerometer with high sensitivity operating in an oscillating circuit", *Journal of microelectromechanical systems*, vol.19, no. 5, pp. 1140-1152, Oct. 2010.

[5] S. A. Zotov, B. R. Simon, A. A. Trusov and A. M. Shkel, "High Quality Factor Resonant MEMS Accelerometer with Continuous Thermal Compensation", *IEEE Sensors Journal*, vol. 15, no. 9, pp. 5045-5052, Sept. 2015.

[6] D. D. Shin, C. H. Ahn, Y.Chen, D. L. Christensen, I. B. Flader, T. W. Kenny, "Environmentally robust differential resonant accelerometer in a wafer-scale encapsulation process", *30th IEEE International Conference on Micro Electro Mechanical Systems (MEMS)*, Las Vegas, 22-26 Jan. 2017, pp 17-20.

[7] I. I. Izyumin, M. H. Kline, Y. C. Yeh, B. Eminoglu, C. H. Ahn, V. A. Hong, Y. Yang, E. J. Ng, T. W. Kenny, and B. E. Boser, "A 7ppm, 6°/hr frequency-output MEMS gyroscope", *28th IEEE International Conference on Micro Electro Mechanical Systems (MEMS)*, Estoril, 18-22 Jan. 2015, pp. 33-36.

[8] V. Zega, P. Minotti, G. Mussi, A. Tocchio, L. Falorni, S. Facchinetti, A. Bonfanti, A. L. Lacaita, C. Comi, G. Langfelder, A. Corigliano, "The First Frequency-Modulated (FM) Pitch Gyroscope", in *Proceedings Eurosensors 2017*, 3-6 September 2017.

[9] P. Minotti, G. Mussi, S. Dellea, A. Bonfanti, A. L. Lacaita, G. Langfelder, A. Tocchio, "A 160 µA, 8 mdps/√Hz frequency-modulated MEMS yaw gyroscope", *IEEE International Symposium on Inertial Sensors and Systems (INERTIAL),* Kawaii, 27-29 Mar. 2017, pp 1-4.

[10] I.I. Izyumin, M. Kline, Y. C. Yeh, B. Eminoglu and B. Boser, "A 50 µW, 2.1 mdeg/s/√ Hz frequency-to-digital converter for frequency-output MEMS gyroscopes", in *European Solid State Circuits Conference (ESSCIRC)*, Venice Lido, 22-26 Sept. 2014 pp. 399-402.

CONTACT

*Cristiano Rocco Marra, cristianorocco.marra@polimi.it